Journal of Power Sources 196 (2011) 5725–5730

Contents lists available at ScienceDirect

Journal of Power Sources

journal homepage: www.elsevier.com/locate/jpowsour

Electrodeposited nanostructured lead dioxide as a thin film electrode for a lightweight lead-acid battery

D.R.P. Egan, C.T.J. Low*, F.C. Walsh

Electrochemical Engineering Laboratory, Energy Technology Research Group, Faculty of Engineering and the Environment, University of Southampton, Highfield, Southampton SO17 1BJ, United Kingdom

ARTICLE INFO

Article history:
Received 9 November 2010
Received in revised form
23 December 2010
Accepted 6 January 2011
Available online 13 January 2011

Keywords:
Deposition
Lead dioxide
Lightweight battery
Methanesulfonic acid
Thin film

ABSTRACT

Thin films of nanostructured lead dioxide are investigated as a positive electrode material for a lightweight lead-acid battery. The films are obtained by constant current deposition from electrolytes of lead methanesulfonate in methanesulfonic acid. The films are tested in two conditions namely (a) cyclic voltammetry and (b) constant current battery cycling in sulfuric acid. The charge and discharge current density, charge density and charge efficiency are measured as a function of cycle number. The effect of deposition conditions, such as solution temperature (295 and 333 K), type of substrate and electrolyte additive (hexadecyltrimethylammonium hydroxide), on the electrochemical performance of the PbO_2 in sulfuric acid is investigated. It is found that the as-deposited lead dioxide film is compact and nanostructured β-phase structure. Following successive cycling in sulfuric acid, the compact thin film gradually transforms into a porous microstructure consisting of positive active material (PbO_2 and $PbSO_4$), several tens of nanometres size. The charge density, discharge density and peak discharge current density of the PbO_2 improve with cycling of the thin film electrode.

1. Introduction

Traditionally, lead-acid batteries have been manufactured by pasted plate technology, which can involve consecutive and time-consuming processes [1,2]. Initially, a flat plate of lead alloy is pressed to form a rectangular open grid. A battery plate is produced by integrating the grid with a lead oxide paste. Curing makes the paste into a cohesive, porous mass and helps bond it to the grid. The battery plates are assembled into a battery and electrically formed to convert their active material into their fully charged condition [3].

An alternative method involves electrodeposition of these active materials directly onto the battery plate. Electrodeposition offers several advantages over pasted plate technology, such as (a) it is a faster method as lead ions, Pb(II), can be directly oxidised to lead dioxide, PbO_2, and reduced to lead, Pb, simultaneously at each electrode [1]; (b) it can be simple to set up and scale up together with a low processing cost; (c) it can facilitate the use of lighter weight substrates as compared to a lead alloy grid [4,5]; (d) single or mixed phase structures of PbO_2 can be readily deposited to exhibit improved electrochemical activity compared to chemically prepared active materials [6].

More recently, methanesulfonic acid has been the choice of aqueous electrolyte for the electrodeposition of lead and lead dioxide. Many investigations have shown that this organic acid offers several advantages over other commodity acids such as it is a less hazardous, more environmentally friendly electrolyte and it has a high solubility for Pb(II) ions [7]. During electrodeposition, Pb^{2+} is oxidised to PbO_2 at the positive electrode, see reaction (1), and Pb^{2+} is reduced to Pb at the negative electrode.

This paper focuses on the electrodeposited lead dioxide. The use of methanesulfonic acid has allowed the deposition of compact and conductive PbO_2 films, which were mechanically stable and adherent to various substrates including reticulated vitreous carbon, nickel and carbon–polymers [8]. The films possessed unique surface properties including high optical surface reflectance [9], nanosized crystallites [10,11] and tailored orthorhombic and tetragonal phase compositions [9,10]:

$$Pb^{2+} + 2H_2O \rightarrow PbO_2 + 4H^+ + 2e^- \quad (1)$$

This paper, for the first time, investigates electrodeposited PbO_2 from methanesulfonic acid and its use as a thin film electrode material in a lightweight lead-acid battery. Different operating parameters were used to deposit the PbO_2 thin films from methanesulfonic acid; the effect of type of substrate, deposition temperature and the use of an electrolyte additive were studied. The electrodeposited PbO_2 films were tested by two methods namely (a) cyclic voltammetry and (b) constant current battery cycling in sulfuric acid, H_2SO_4. The results from the recorded cyclic voltammograms

* Corresponding author. Tel.: +44 0 23 8059 7052; fax: +44 0 23 8059 7051.
E-mail address: C.T.J.Low@soton.ac.uk (C.T.J. Low).

0378-7753/$ – see front matter.
doi:10.1016/j.jpowsour.2011.01.008

were compared to investigate the effect the different deposition conditions have on the cycling behaviour of the PbO_2 in sulfuric acid.

2. Experimental details

2.1. Electrodeposition of lead and lead dioxide thin films

Lead and lead dioxide films were electrodeposited from an electrolyte of 0.5 mol dm^{-3} lead(II) methanesulfonate, $Pb(CH_3SO_3)_2$, and 0.5 mol dm^{-3} methanesulfonic acid, CH_3SO_3H, in an undivided parallel plate, 'beaker' cell. The film thickness and mass of the of the lead dioxide film were 48 μm and 0.892 g, respectively, as calculated using Faraday's Law. The film thickness was 34 μm for lead. Different operating conditions were used to electrodeposit the lead and lead dioxide thin films. These included testing two different electrolyte temperatures: 295 and 333 K. Different concentrations of the additive, hexadecyltrimethylammonium hydroxide ($C_{19}H_{43}NO$), in the electrolyte were examined: 0.0, 1.0 and 5.0 mmol dm^{-3}. Three different materials were used as substrates for the PbO_2 films; nickel, graphite and carbon–polymer solid rectangular plates (area, 4 cm × 5 cm). The carbon–polymer was a carbon–polyvinyl–ester composite (BMC 940) supplied by Entegris Fuel Cells.

Prior to electrodeposition, the substrate was dry polished with silicon carbide paper down to grade P1200 and cleaned ultrasonically in ultra pure water for 2 min, washed with Teepol multipurpose detergent, followed by a further 2 min ultrasonic clean. The back and sides of the substrate were covered with green polyester tape (Cole Parmer Instrument Co.). A constant current density, 20 mA cm^{-2}, was applied and the deposition was carried out for 1800 s. The electrolyte volume was approximately 260 cm^3. A magnetic stirrer (PTFE-coated steel cylindrical stirrer bar, 2.5 cm length and 0.65 cm diameter), rotated at 300 rpm, was used to generate flow in the solution.

2.2. Cyclic voltammetry of the thin films in sulfuric acid

Following electrodeposition, the 'as-deposited' PbO_2 films were evaluated via cyclic voltammetry in 4.0 and 4.7 mol dm^{-3} sulfuric acid under static conditions and at room temperature, 295 K. Cyclic voltammetry was performed in a three-electrode glass cell. A platinum mesh (area, 1 cm^2) was used as the counter electrode. All electrode potentials were measured against a saturated calomel electrode, SCE in 3.5 mol dm^{-3} KCl. All electrochemical measurements were made with an EcoChemie Autolab (PGSTAT20) computer controlled potentiostat using the General Purpose, Electrochemical Software (GPES) Version 4.5. All chemicals were analytical reagent grade from Sigma Aldrich UK. The potential was swept between 1 and 2 V *vs.* SCE at a sweep rate of 10 mV s^{-1} [6,12].

2.3. Cycling of thin-film electrodes in a lead-acid battery

A lead-acid battery was tested under static conditions at 295 K. The battery consisted of a single cell: constructed from the 'as-deposited' Pb and PbO_2 thin film electrodes on nickel substrates. The films were electrodeposited from a solution containing 0.5 mol dm^{-3} $Pb(CH_3SO_3)_2$ and 0.5 mol dm^{-3} CH_3SO_3H. Deposition was carried out at 20 mA cm^{-2} for 1800 s in a stirred solution at 333 K. The electrolyte for battery testing was 100 mL of 4.0 mol dm^{-3} H_2SO_4 contained in a glass beaker. The electrodes were placed parallel facing each other in the beaker and the inter-electrode gap was about 5 mm. The active area of each of the electrodes was approximately 3 cm × 4 cm. The battery cell was cycled using a BA400 Battery Analyzer, LaMantia Products Ltd., Canada and the data was logged with National Instruments Measurement and Automation Software, United Kingdom.

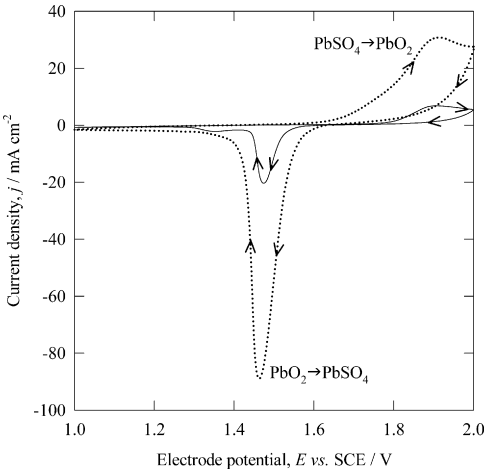

Fig. 1. Cyclic voltammograms of an electrodeposited PbO_2 thin film in 4.7 mol dm^{-3} sulfuric acid under static conditions at 295 K. Active area 2.3 cm2. A platinum mesh counter electrode was used. The potential was swept at 10 mV s^{-1}. PbO_2 was anodically deposited onto a nickel substrate from a solution containing 0.5 mol dm^{-3} $Pb(CH_3SO_3)_2$, 0.5 mol dm^{-3} CH_3SO_3H and 1.0 mmol m^{-3} $C_{19}H_{43}NO$. Deposition was carried out at 20 mA cm^{-2} for 1800 s in a stirred solution at 333 K. Cycle 10 and Cycle 200.

2.4. Microstructural characterisation

Surface microstructure characterisation was carried out using a high resolution scanning electron microscope, JEOL JSM 6500F. An accelerating voltage of 15 kV was used and the imaging was carried out with a working distance of approximately 10 mm.

3. Results and discussion

3.1. Cycling in H_2SO_4 with a three-electrode cell

Fig. 1 shows the recorded cyclic voltammograms on a PbO_2 film in 4.7 mol dm^{-3} H_2SO_4. The PbO_2 film was electrodeposited from a solution containing 0.5 mol dm^{-3} $Pb(CH_3SO_3)_2$, 0.5 mol dm^{-3} CH_3SO_3H and 1.0 mmol dm^{-3} $C_{19}H_{43}NO$. The cyclic voltammograms showed typical oxidation and reduction peaks essentially similar to those previously reported in the literature [6,12,13].

During the anodic scan of the first cycle, increasing the potential from +1 to +2 V *vs.* SCE resulted in oxygen evolution on the PbO_2 film. During the cathodic scan, as the electrode potential was decreased back to +1 V *vs.* SCE, lead dioxide was reduced to lead sulfate at +1.47 V *vs.* SCE, see Eq. (2). In the anodic scans of subsequent cycles, this lead sulfate, $PbSO_4$, was re-oxidised to PbO_2 at +1.89 V *vs.* SCE. Comparing the two cycles shown in Fig. 1, in cycle 200 the peak charge and discharge current density were greater. The potentials, at which the peak current densities occurred, remained unchanged as the PbO_2 film was cycled. The swept areas of the anodic and cathodic parts of the cyclic voltammogram were also greater in cycle 200, indicating an increase in both the charge and discharge density.

$$PbO_2 + 4H^+ + 2e^- + SO_4^{2-} \underset{\text{charge}}{\overset{\text{discharge}}{\rightleftharpoons}} PbSO_4 + 2H_2O$$

$$E^e = +1.45\,\text{V}\ vs.\ \text{SCE} \qquad (2)$$

The charge density, discharge density and peak current density of the PbO_2 film were recorded from the cyclic voltammograms. For a given cycle, the charge density during charge was found by

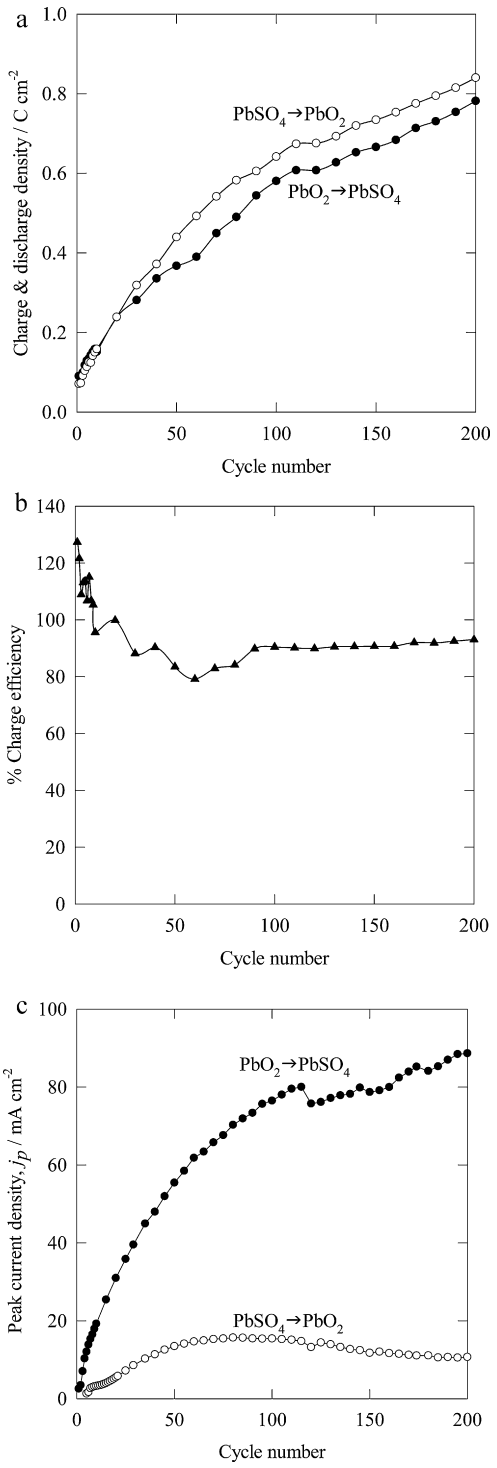

Fig. 2. Electrochemical data for a PbO_2 thin film cycled in 4.7 mol dm^{-3} H_2SO_4. (a) Charge and discharge density, (b) charge efficiency ▲ and (c) peak current density. ● Discharge cycle. ○ Charge cycle. Cycling was carried out under static conditions at 295 K, with an active area of 2.3 cm^2. The potential was swept at 10 mV s^{-1}. PbO_2 was anodically deposited onto nickel from a solution containing 0.5 mol dm^{-3} $Pb(CH_3SO_3)_2$, 0.5 mol dm^{-3} CH_3SO_3H and 1.0 mmol dm-3 $C_{19}H_{43}NO$. Deposition was carried out at 20 mA cm^{-2} for 1800 s in a stirred solution at 333 K.

calculating the area under the anodic peak,of the j vs. E curve, and dividing it by the scan rate. Similarly, discharge density was found from the area under the cathodic peak. The results are presented as a function of cycle number in Fig. 2. Fig. 2(a) shows that, for the first 9 cycles, the discharge density of the PbO_2 film was greater than its charge density due to the lack of $PbSO_4$ to re-oxidise to PbO_2. This explains why the charge efficiencies were greater than 100%, see Fig. 2(b). By cycle 90 the charge and discharge density increased at similar rates which resulted in the charge efficiency stabilising at 90%, see Fig. 2(b).

Fig. 2(c) shows the peak current density during charge increased with the number of cycles. The relationship reached a maxima point. Further cycling of the electrode material led to a decrease in the peak charge current density followed by a plateau off at higher cycles.

Fig. 2(a) and (c) shows the charge density, discharge density and peak discharge current density of the PbO_2 film increased with cycling. These trends were observed in all cyclic voltammetry tests on the PbO_2 thin films in sulfuric acid. They are a common feature of lead-acid cells with all types of electrodes, at least during the initial cycles [5,14].

3.1.1. *Surface microstructure of PbO_2/$PbSO_4$*

Scanning electron microscopy was used to image the surface microstructure of the positive active material, PbO_2/$PbSO_4$, to explain for the increase in charge density, discharge density and peak discharge current density of the PbO_2 film with cycling in sulfuric acid. As deposited, the PbO_2 film was compact with good adhesion to the nickel substrate, see Fig. 3(a). Its surface was composed of pyramidal like structures [10,11]. After 10 cycles, Fig. 3(b), it changed from a compact to a macroporous coating. After 200 cycles, Fig. 3(c), its porosity further increased and its microstructure changed into a highly porous one with nano-sized particles. The images showed that the porosity of the film increased with cycling while the size of the film particles decreased to several tens of nanometres.

As the size of the surface particles reduced with cycling, the electrode surface area became enlarged. There was subsequently more active material on which the electrochemical reactions could take place [3,15]. As the porosity of the film increased with cycling, the contact area between the active material and the electrolyte grew. This allowed for greater diffusion of H^+ ions into the film making it easier for the reduction of PbO_2 to $PbSO_4$ [12,16,17]. Although the porosity of the PbO_2 film increased with cycling, it was still sufficiently thick to prevent corrosion of the nickel substrate by sulfuric acid.

3.2. *Effect of substrate on the cycling of PbO_2 thin films in sulfuric acid*

In this work, PbO_2 films were electrodeposited onto three different substrates: carbon–polymer, nickel and graphite solid rectangular plates. These lightweight substrates help to achieve weight savings in the lead-acid battery by replacing the lead alloy grid as the current collector. The three films were each deposited from a solution containing 0.5 mol dm^{-3} $Pb(CH_3SO_3)_2$ and 0.5 mol dm^{-3} CH_3SO_3H. Electrodeposition was carried out for a duration of 1800 s at 20 mA cm^{-2} in a stirred solution at 333 K. The PbO_2 thin film adhered to the nickel and formed a grey uniform, compact coating [18]. The three electrodeposited PbO_2 films were tested via cyclic voltammetry in 4.0 mol dm^{-3} H_2SO_4. Cycling was carried out using a glass three-electrode cell over an area of 2 cm^2. The results for the three films are compared below, to examine the effect of substrate material on the cycling of the PbO_2 films in sulfuric acid.

The PbO_2 thin film on the carbon–polymer failed and came away from the surface while cycling in 4.0 mol dm^{-3} H_2SO_4. For the first 20 cycles its charge efficiency fluctuated between 83 and 86%, after which it declined due to increasing oxygen evolution. Its charge efficiency was 31% at cycle 50, see Table 1. It has been reported that glassy carbon was poor for the conversion of Pb^{2+} to PbO_2 from a solution containing 0.3 mol dm^{-3} $Pb(CH_3SO_3)_2$ and 1 mol dm^{-3}

Table 1
Influence of electrodeposition operating conditions on the charge and discharge cycle performance of PbO_2 thin films in H_2SO_4 at 295 K. Films deposited from solutions containing the additive were cycled in 4.7 mol dm^{-3} H_2SO_4. All others were cycled in 4.0 mol dm^{-3} H_2SO_4. Unless otherwise stated, PbO_2 was anodically deposited onto nickel at 20 mA cm^{-2} for 1800 s under stirred conditions at 333 K and the deposition electrolyte contained 0.5 mol dm^{-3} Pb $(CH_3SO_3)_2$ and 0.5 mol dm^{-3} CH_3SO_3H. For the tests examining the effect of temperature, 5 mol dm^{-3} $C_{19}H_{43}NO$ was added to this electrolyte.

Cycle number from cyclic voltammogram	Electrodeposition operating conditions	Peak current density/mA cm-2		Charge and discharge density / C cm-2		% Charge efficiency
		Charge	Discharge	Charge	Discharge	
Concentration of $C_{19}H_{43}NO$ in electrolyte						
80	0.0 mol dm^{-3}	25	125	1.44	1.25	87
	0.001 mol dm^{-3}	15	70	0.58	0.49	84
	0.005 mol dm^{-3}	19	80	0.62	0.61	98
Electrolyte temperature						
28	295 K	9	47	0.56	0.32	58
	333 K	10	44	0.32	0.31	97
Type of substrate						
50	Carbon-polymer	10	55	3.91	1.20	31
	Nickel	23	104	1.02	0.96	94

CH_3SO_3H [19]. Others found that vitreous carbon was inferior to nickel substrate for the long term adhesion of PbO_2 deposits in a lead-acid flow cell employing lead(II) dissolved in methanesulfonic acid [20]. The failure of the PbO_2 film on the carbon–polymer substrate could also have been due to the observed oxygen evolution on the positive electrode during electrodeposition. Some of the applied current was then spent in the oxygen evolution reaction, instead of the preparation of a uniform PbO_2 film [21]. The formed oxygen may have also created cracks in the PbO_2 film during deposition [22].

The PbO_2 film on the graphite substrate also failed and there was material loss in the form of carbon particles coming off the graphite. Previously it has been reported that graphite foam was electrochemically unstable in the voltage range where the positive electrode operates [23]. This was because of the intercalation of sulfuric acid into the graphite, whereby the graphite oxidises to form graphite–sulfuric acid intercalation compounds [23]. Therefore graphite is not a suitable substrate for the lead dioxide electrode of a lead acid battery [23].

Only the PbO_2 thin film deposited on nickel was stable while cycling in sulfuric acid. It was observed that, after being left at open-circuit for 3 days, the PbO_2 film on nickel did not cycle; it self-discharged and became passivated by lead sulfate. The PbO_2 film on nickel yielded higher peak discharge current densities and charge efficiencies than the PbO_2 film on the carbon–polymer, see Table 1.

3.3. *Effect of deposition temperature on the cycling of PbO_2 thin films in sulfuric acid*

Two PbO_2 thin films were each electrodeposited onto nickel from a solution containing 0.5 mol dm^{-3} $Pb(CH_3SO_3)_2$, 5.0 mmol dm^{-3} hexadecyltrimethylammonium hydroxide ($C_{19}H_{43}NO$) (Fluka) and 0.5 mol dm^{-3} CH_3SO_3H. One film was electrodeposited at 295 K while the other was electrodeposited at 333 K. The PbO_2 film deposited at 295 K was of the α phase [9,10]. It was uniform, black and highly reflective [8,9,18]. The high reflectivity was due to the flat and very smooth characteristics of α-PbO_2 films [10]. The PbO_2 thin films formed at 333 K were of the β phase and were matte grey and compact [10,11].

Cyclic voltammetry was carried out on the two PbO_2 films in 4.7 mol dm^{-3} H_2SO_4 in a glass three-electrode cell over an area of 2.3 cm^2. The PbO_2 thin film deposited at 295 K failed and came away from the nickel. It failed because of its morphology, α-PbO_2 [9,18]: α-PbO_2 has a more compact structure than β-PbO_2 which makes α-PbO_2 more difficult to discharge compared to β-PbO_2 [24,25]. The compactness of the α-PbO_2 film meant it was susceptible to cracking as a result of the volume expansion during the reduction of PbO_2 to $PbSO_4$. β-PbO_2 is the preferred form for industrial applications because its highly porous structure allows high current densities to be obtained [6,26]. The high porosity accommodated the volume expansion during the reduction of PbO_2 to $PbSO_4$ [3,6,23,26]. The charge efficiency was higher for the PbO_2 film deposited at 333 K (97%) than it was for the one deposited at 295 K (58%), as shown in Table 1.

In another set of tests, involving two PbO_2 thin films electrodeposited onto carbon–polymer substrates at different temperatures, the potential during the electrodeposition at 333 K was lower (2.17 V) than it was at 295 K (2.46 V). This was because of the higher conductivity of the electrolyte and improved electrode kinetics at the elevated temperature [18,27].

3.4. *Effect of additive concentration on the cycling of PbO_2 thin films in sulfuric acid*

Three PbO_2 films were electrodeposited onto nickel substrates from a solution containing 0.5 mol dm^{-3} lead(II) methanesulfonate, 0.5 mol dm^{-3} methanesulfonic acid and the additive, hexadecyltrimethylammonium hydroxide, $C_{19}H_{43}NO$. Three different concentrations of the additive were investigated: 0.0, 1.0 and 5.0 mmol dm^{-3}. Electrodeposition was carried out at a current density of 20 mA cm^{-2} for 1800 s in a stirred solution at 333 K. The three PbO_2 films were matte-grey in appearance, compact, non-dendritic and well-adherent to the substrate. The additive had little effect on the macro-visual appearance of the PbO_2 thin films [18]. The deposited PbO_2 films were β-phase in agreement with other work [9,18]. The as-deposited Pb film was silvery and without the use of additive in the deposition electrolyte, it appeared porous and did not adhere well to the nickel substrate [8,28].

The three PbO_2 films were then tested using cyclic voltammetry in H_2SO_4. The PbO_2 film deposited from the solution without the additive was cycled in 4.0 mol dm^{-3} H_2SO_4 with an active area of 2.0 cm^2. The two PbO_2 films deposited from the solutions containing the additive were cycled in 4.7 mol dm^{-3} H_2SO_4, each with an active area of 2.3 cm^2. Table 1 shows that the additive affected the cycling performance of the PbO_2 films. Of the three PbO_2 films, the one deposited from the additive free solution yielded the highest current, charge and discharge densities. This was because the additive could have increased the compactness of these films resulting in less active mass being available for the electrochemical reactions. The PbO_2 film deposited from the solution with 5 mmol dm^{-3} $C_{19}H_{43}NO$ yielded the highest charge efficiency of 98%. The PbO2 film deposited from a solution with 1 mmol dm^{-3} $C_{19}H_{43}NO$ yielded the lowest current, charge and discharge densities.

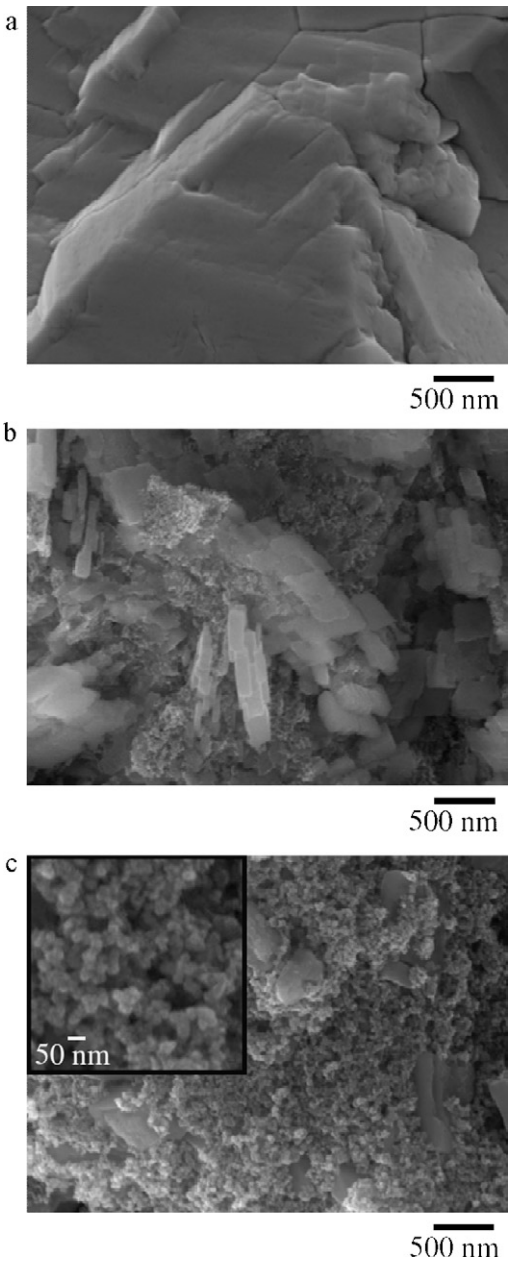

Fig. 3. Surface morphology of PbO_2 (a) as-deposited, (b) after 10 cycles and (c) after 200 cycles in 4.7 mol dm^{-3} H_2SO_4. Inset in (c) shows highly porous, nanostructured $PbSO_4/PbO_2$ positive active materials. PbO_2 was anodically deposited onto a nickel substrate from a solution containing 0.5 mol dm^{-3} $Pb(CH_3SO_3)_2$, 0.5 mol dm^{-3} CH3SO3H and 1.0 mmol dm^{-3} $C_{19}H_{43}NO$. Deposition was carried out at 20 mA cm^{-2} for 1800 s in a stirred solution at 333 K.

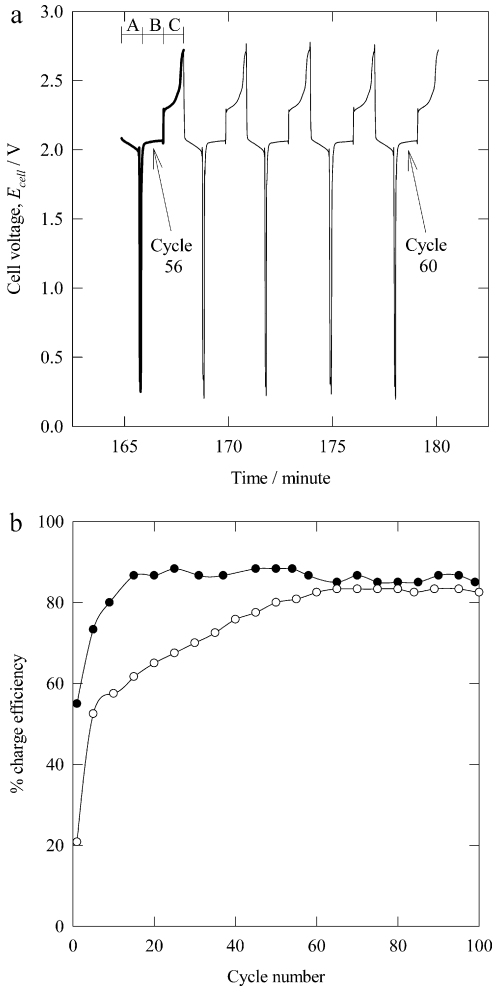

Fig. 4. Charge-discharge data for electrodeposited Pb and PbO_2 thin film electrodes in a lead-acid battery. (a) charge-discharge cycles in 4.0 mol dm^{-3} H_2SO_4 (100 mL) at 295 K. The battery cycled at a constant current density of 10 mA cm^{-2}. Charge time of 60 s. A = discharge, B = open-circuit and C = charge of cycle 56. Cut-off for discharge voltage, 1 V. (b) Charge efficiency of the cell for two different current densities ● 10 mA cm^{-2} (charge time 60 s); ○ 20 mA cm^{-2} (charge time 120 s). The thin films of lead (34 μm) and lead dioxide (48 μm) were deposited onto nickel substrates from a solution containing 0.5 mol dm^{-3} $Pb(CH_3SO_3)_2$ and 0.5 mol dm^{-3} CH_3SO_3H. Electrodeposition was carried out at 20 mA cm^{-2} in a stirred solution at 333 K. The active area of each of electrodes in the lead-acid battery was 3 cm × 4 cm.

3.5. Charge–discharge of thin-film electrodes in a lead-acid battery

A lead-acid battery was tested under static conditions at 295 K. The battery consisted of a single cell made up of Pb and PbO_2 thin film electrodes immersed in 100 mL of 4.0 mol dm^{-3} H_2SO_4 in a glass beaker. The Pb and PbO_2 films were on nickel substrates. The cell was cycled at two different current densities: 10 and 20 mA cm^{-2}. In both cases the discharge cut-off voltage was set to 1 V. Initially the cell was discharged at 10 mA cm^{-2}, then held at open-circuit for 60 s and charged at 10 mA cm^{-2} for a further 60 s. This cycle was repeated 100 times. The electrodes were then removed from the electrolyte for a period of time. Upon replacement of the electrodes back into the same electrolyte, the cell was cycled for a further 200 cycles at 20 mA cm^{-2}, with open-circuit and charge times set to 60 s and 120 s, respectively.

Fig. 4(a) shows the cell voltage *vs.* service time at 10 mA cm^{-2}. Examining cycle 56 in Fig. 4(a), the charge cell voltage increased with time, starting at 2.27 V and climbing to 2.72 V before discharge. There are many reasons for the high cell voltage at the end of the charge cycle, e.g. (a) an increase in the electrode resistivity due to the insulating property of $PbSO_4$, (b) oxygen evolution reaction at the active sites of positive active material and (c) changes in the local surface pH and conductivity.

The increase in charge voltage with charge time decreased as cycling progressed which indicates a valuable improvement in battery performance [27]. At both current densities, the average charge voltage decreased with cycling and reached a plateau faster at 10 mA cm^{-2} than it did at 20 mA cm^{-2}. At 10 mA cm^{-2}, the average charge voltage stabilised at 2.41 V by cycle 28. At 20 mA cm^{-2}, the average charge voltage stabilised at 2.42 V by cycle 85. The voltage and energy efficiency while cycling at 10 mA cm^{-2} (84% and 73%, respectively at cycle 95) were higher than they were when cycling at 20 mA cm^{-2} (80% and 66%, respectively at cycle

95). These efficiency values were recorded at cycle 95 in both cases.

Fig. 4(b) shows the variation of charge efficiency with cycling for the thin-film lead-acid battery. At 10 mA cm^{-2}, the discharge time stabilised at 51 s giving a charge efficiency of 85% and a discharge density of 0.14 mA h cm^{-2}. This is lower than the charge density of 10 mA h cm^{-2} passed during the electrodeposition of the thin film electrodes. At 10 mA cm^{-2}, the cell discharged at 2 V, yielding an energy density of 0.28 mW h cm^{-2} and power density of 20 mW cm^{-2}. While cycling at 20 mA cm^{-2}, the charge time was increased from 60 to 120 s. The discharge time then increased from 51 to 100 s, giving a charge efficiency of 83% and a discharge density of 0.55 mA h cm^{-2}. The discharge cell voltage was 1.9 V, yielding an energy density was 1.05 mW h cm^{-2} and power density of 38 mW cm^{-2}. Fig. 4(b) shows that during the initial battery cycles the charge efficiency increased with cycling. This can be explained by the increases observed in the charge and discharge densities of the Pb and PbO_2 films while carrying out the cyclic voltammetry tests in sulfuric acid.

After 100 cycles at 10 mA cm^{-2}, both films were still intact on the nickel substrates. After the further 200 cycles at 20 mA cm^{-2}, the Pb film came away from its nickel substrate. There were grey particles suspended in the electrolyte and the electrolyte had a green discolouration due to corrosion of the nickel substrate of the negative electrode [29].

4. Conclusions

1. PbO_2 thin film were electrodeposited from methanesulfonic acid and used as electrodes for a lightweight lead-acid battery in sulfuric acid at 295 K.
2. As deposited, PbO_2 film was compact and adherent to the nickel substrate. After successive cycling of the film in sulfuric acid, it transformed into a microporous structure composed of nano-sized particles. This transformation explained the film's increasing discharge density and peak discharge current density with cycling. The highest values obtained were 1.25 C cm^{-2} and 125 mA cm^{-2}.
3. A lead-acid battery consisting of thin film lead and lead dioxide electrodes was cycled at 10 and 20 mA cm^{-2}, achieving discharge densities of 0.51 and 2 C cm^{-2}, respectively.
4. The operating parameters used to deposit the PbO_2 thin film influenced its charge and discharge performance in a half-cell in sulfuric acid. PbO_2 film, on nickel, electrodeposited at 333 K cycled for a longer duration in sulfuric acid than that deposited at 295 K. The PbO_2 film electrodeposited at 295 K failed and came away from the nickel substrate during cycling.
5. PbO_2 thin film was more stable on nickel substrate, while cycling in sulfuric acid, than on carbon–polymer and graphite substrates.
6. PbO_2 electrodeposited from a solution without the $C_{19}H_{43}NO$ additive, yielded higher current and higher charge and discharge densities while cycling in sulfuric acid than those deposited from a solution with the additive.

Acknowledgement

This work formed part of D.R.P. Egan's research dissertation project for the MSc in Sustainable Energy Technologies at the University of Southampton.

References

[1] D. Linden, T.B. Reddy, Handbook of Batteries, 3rd ed., McGraw-Hill, 2001.
[2] H. Dahodwalla, S. Herat, J. Clean. Prod. 8 (2000) 133–142.
[3] C.A. Vincent, B. Scrosati, Modern Batteries: An Introduction to Electrochemical Power Sources, 2nd ed., Butterworth-Heinemann, 2003.
[4] K. Das, A. Mondal, J. Power Sources 55 (1995) 251–254.
[5] K. Das, A. Mondal, J. Power Sources 89 (2000) 112–116.
[6] D. Devilliers, M.T. Dinh Thi, E. Mahé, V. Dauriac, N. Lequeux, J. Electroanal. Chem. 573 (2004) 227–239.
[7] M.D. Gernon, M. Wu, T. Buszta, P. Janney, Green Chem. 1 (1999) 127–140.
[8] D. Pletcher, H. Zhou, G. Kear, C.T.J. Low, F.C. Walsh, R.G.A. Wills, J. Power Sources 180 (2008) 630–634.
[9] C.T.J. Low, D. Pletcher, F.C. Walsh, Electrochem. Commun. 11 (2009) 1301–1304.
[10] I. Sirés, C.T.J. Low, C. Ponce-de-León, F.C. Walsh, Electrochim. Acta 55 (2010) 2163–2172.
[11] I. Sirés, C.T.J. Low, C. Ponce-de-León, F.C. Walsh, Electrochem. Commun. 12 (2010) 70–74.
[12] D. Zhou, L. Gao, Electrochim. Acta 53 (2007) 2060–2064.
[13] N. Yu, L. Gao, Electrochem. Commun. 11 (2009) 220–222.
[14] M. Dimitrov, D. Pavlov, J. Power Sources 93 (2001) 234–257.
[15] Z. Shi, H. Zhan, Y.-H. Zhou, C.-S. Cha, J. Power Sources 62 (1996) 135–139.
[16] E.E. Ferg, P. Loyson, N. Rust, J. Power Sources 141 (2005) 316–325.
[17] S. Ghasemi, M.F. Mousavi, H. Karami, M. Shamsipur, S.H. Kazemi, Electrochim. Acta 52 (2006) 1596–1602.
[18] X. Li, D. Pletcher, F.C. Walsh, Electrochim. Acta 54 (2009) 4688–4695.
[19] H.Y. Peng, H.Y. Chen, W.S. Li, S.J. Hu, H. Li, J.M. Nan, Z.H. Xu, J. Power Sources 168 (2007) 105–109.
[20] A. Hazza, D. Pletcher, R. Wills, Phys. Chem. Chem. Phys. 6 (2004) 1773–1778.
[21] S. Ghasemi, M.F. Mousavi, M. Shamsipur, Electrochim. Acta 53 (2007) 459–467.
[22] M. Ghaemi, E. Ghafouri, J. Neshati, J. Power Sources 157 (2006) 550–562.
[23] Y.-I. Jang, N.J. Dudney, T.N. Tiegs, J.W. Klett, J. Power Sources 161 (2006) 1392–1399.
[24] P.K. Shen, X.L. Wei, Electrochim. Acta 48 (2003) 1743–1747.
[25] I. Petersson, E. Ahlberg, B. Berghult, J. Power Sources 76 (1998) 98–105.
[26] F. Scholz, C. Pickett, Encyclopedia of Electrochemistry: Inorganic Electrochemistry, Wiley-VCH, 2006.
[27] D. Pletcher, R. Wills, Phys. Chem. Chem. Phys. 6 (2004) 1779–1785.
[28] D. Pletcher, H. Zhou, G. Kear, C.T.J. Low, F.C. Walsh, R.G.A. Wills, J. Power Sources 180 (2008) 621–629.
[29] E. Volkova, A. Demidov, Russ. J. Appl. Chem. 82 (2009) 337–339.